Molecular Mechanisms of Resveratrol Action in Lung Cancer Cells Using Dual Protein and Microarray Analyses

Lorna Whyte, Yuan-Yen Huang, Karen Torres, and Rajendra G. Mehta

Carcinogenesis and Chemoprevention Division, IIT Research Institute, Chicago, Illinois

Abstract

Resveratrol, a natural phytoestrogen found in red wine and a variety of plants, is reported to have protective effects against lung cancer; however, there is little work directed toward the understanding of the mechanism of its action in this disease. In this study, we used a combination of experimental approaches to understand the biological activity and molecular mechanisms of resveratrol. Microarray gene expression profiling and high-throughput immunoblotting (PowerBlot) methodologies were employed to gain insights into the molecular mechanisms of resveratrol action in human lung cancer cells. In this report, we confirm the up-regulation of p53 and p21 and the induction of apoptosis by the activation of the caspases and the disruption of the mitochondrial membrane complex. We show the arrest of A549 cells in the G_1 phase of cell cycle in the presence of resveratrol and also report alterations in both gene and protein expressions of cyclin A, chk1, CDC27, and Eg5. Furthermore, the results indicated that resveratrol action is mediated via the transforming growth factor-β pathway, particularly through the Smad proteins. Results showed the down-regulation of the Smad activators 2 and 4 and the up-regulation of the repressor Smad 7 as a result of resveratrol treatment. Resveratrol is a potent inhibitor of A549 lung cancer cell growth, and our results suggest that resveratrol may be a promising chemopreventive or chemotherapeutic agent for lung cancer. [Cancer Res 2007;67(24):12007–17]

Introduction

Resveratrol (3,5,4′-trihydroxy-stilbene) is a phytoalexin found in red wine and a variety of plants, including grapes, peanuts, mulberries, and legumes (1). Phytoalexins are produced in response to stress, injury, fungal infection, or UV exposure (1, 2). Resveratrol is found in both the *trans-* and the *cis*-isomeric forms, although *trans*-resveratrol is thought to be the biologically active isoform due to steric stability (3). The biological importance of resveratrol first emerged when it was found present in red wine and was found to be used in traditional Chinese and Japanese medicine (4). Many studies have been published to date demonstrating the beneficial effects of resveratrol in cellular systems. Epidemiologic studies revealed an inverse correlation between red wine consumption and cardiovascular disease in France (known as the "French Paradox") (5). Other studies have shown resveratrol to be associated with lipids and to inhibit lipid oxidation (6, 7). Additionally, resveratrol has been found to inhibit platelet aggregation (8) and also to have antioxidant properties (9).

During the past 25 years, studies on identifying cancer-chemopreventive agents have received considerable attention. Numerous natural and synthetic chemopreventive agents have been established as a result of their efficacy in experimental carcinogenesis models (10). In the first report of resveratrol as a possible cancer chemopreventive agent, Jang et al. (11) reported that resveratrol exerts antitumor properties at all three stages of skin carcinogenesis, including initiation, promotion, and progression. Since then, other studies have confirmed this work, and resveratrol has been shown to have chemopreventive properties in many cancer types, including mammary, prostate, colon, and lung carcinogenesis (12–15). Its role in prevention and therapy of cancers of several target organs has been extensively reviewed (1, 16–19).

Interestingly, an epidemiologic study has recently reported that high intake of beer or spirits is correlated with increased relative risk of lung cancer, whereas consumption of red wine is correlated with a reduced risk (20). This protective effect is attributed to resveratrol and flavonoids present in red wine. Resveratrol has already been established as an antiproliferative agent in A549 human lung cancer cells, and this effect has been correlated with the suppression of phosphorylation of Rb protein and transcription factors such as nuclear factor-κB (NF-κB) and activator protein-1 (AP-1) (21). Kim et al. also showed that this suppression is accompanied with the induction of p21WAF1/CIP and an increased activity of caspase-3, which results in increased apoptosis. In human epidermoid A431 cells, resveratrol treatment resulted in growth arrest in G_1 (22). Consistent with the results reported for lung cancer, in these cells, induction of p21/WAF1 was observed. Despite these promising leads, there is very little work directed toward understanding the mechanism of action of resveratrol in lung cancer.

In the present study, we orchestrated a dual/combined experimental approach to identify novel mechanisms of resveratrol action in human lung cancer A549 cells. We compiled gene expression profiles using a cDNA microarray and altered expression of proteins as a result of resveratrol treatment using a high-throughput immunoblotting technique known as PowerBlot. Analyses of these data provided new insights into the molecular mechanisms of resveratrol action on lung cancer. To our knowledge, this is the first report that uses the dual microarray—PowerBlot approach to match gene and protein alterations to elucidate mechanisms of action of resveratrol in lung cancer prevention/therapy.

Materials and Methods

Cell line and reagents. The human lung carcinoma cell lines A549, NCI H460, and NCI H23 were obtained from the American Type Culture Collection and cultured according to the supplier's recommendations. The

cells were maintained at 37°C with 5% CO_2 in a humidified atmosphere and routinely passaged twice to thrice per week. Resveratrol was obtained from the National Cancer Institute. For experimental use, resveratrol was dissolved in ethanol with concentrations in the media not exceeding 0.1%.

Cell proliferation studies. Cells were seeded (5,000 cells per well) in 24-well plates (Corning Inc.) and treated with ethanol (control) or resveratrol for the indicated times and dosages. Crystal violet assays were used to measure cell growth. After treatment, the cells were fixed in 1% glutaraldehyde for 15 min at room temperature. Crystal violet solution (0.1%) was added and incubated for 30 min at room temperature. Excess dye was discarded, and 0.2% Triton X-100 was added to each well. Absorbance was measured at A590 using a microplate reader.

Cell cycle analysis. For DNA content analysis, A549 cells were treated with ethanol (control) or with resveratrol (25 μmol/L) for 48 h. The cells were fixed in ice-cold 70% ethanol at the end of the treatment. The nuclei were prepared for DNA analysis as previously described (23). Briefly, the cells were washed in PBS and suspended in citrate buffer [250 mmol/L sucrose, 40 mmol/L trisodium citrate, 0.05% DMSO (pH, 7.6)]. The nuclei were trypsinized with buffer containing 1.5 mmol/L spermine tetrahydrochloride, 0.1% NP40, 3.4 mmol/L trisodium citrate, 0.5 mmol/L trizma, and 0.3 mg/mL trypsin (pH, 7.6). Before propidium iodide (0.416 mg/mL) staining, proteolysis was stopped with buffer containing trypsin inhibitor (0.25 mg/mL) and 0.1 mg/mL RNase A. Preparations were then analyzed by fluorescence-activated cell sorting (FACS) analysis.

Terminal nucleotidyl transferase–mediated nick end labeling assay. A549 cells were seeded (5,000 cells per chamber) on poly–L-lysine–coated Lab-Tek II Chamber slides (Nalge Nunc International) and treated with ethanol control or resveratrol (25 μmol/L) for 48 h. Following the treatment, the cells were washed with PBS, fixed in 3.7% formaldehyde for 10 min at room temperature, and permeablized in 100% methanol for 6 min at −20°C. DNA fragmentation was detected immunohistochemically using the *In situ* Cell Death Detection-POD kit (Roche) as per manufacturer's instructions.

Poly caspase FLICA. Cells were seeded and treated on poly–L-lysine–coated Lab-Tek II Chamber slides as above. The poly caspase FLICA assay was done as per manufacturer's instructions (Immunohistochemistry Technologies, LLC). Briefly, following treatment, cells were incubated with the poly caspase FLICA reagent for 1 h at 37°C and 5% CO_2 and analyzed directly under a fluorescence microscope to view the green fluorescence of caspase-positive cells.

Mito-PT assay. Cells were seeded and treated on poly–L-lysine–coated Lab-Tek II Chamber slides as above. The Mito-PT assay was done as per manufacturer's instructions (Immunohistochemistry Technologies, LLC). Briefly, following treatment, cells were incubated with the Mito-PT reagent for 15 min at 37°C and 5% CO_2 and analyzed directly under a fluorescence microscope to view changes in the mitochondrial permeability transition as indicated by the red fluorescence in the cells.

Western blotting. A549 cells were treated with ethanol (control) or 25 μmol/L resveratrol for 48, 72, and 96 h. Cells were lysed at each time point with 1× radioimmunoprecipitation assay buffer (RIPA; 1× TBS, 1% NP40, 0.5% sodium deoxycholate, 0.1% SDS, 0.004% sodium azide; Santa Cruz Biotechnology) supplemented with protease inhibitor cocktail, 2 mmol/L phenylmethylsulfonyl fluoride, and 1 mmol/L sodium orthovanadate (Santa Cruz Biotechnology). Cell lysates were analyzed using the Lowry protein assay (Bio-Rad). Proteins were separated by 10% SDS-PAGE, transferred to nitrocellulose membranes, and probed with mouse monoclonal p53 (1:1,000 dilution; Ab-6, Oncogene), rabbit polyclonal p21 (1:200 dilution; C-19, Santa Cruz Biotechnology) or rabbit polyclonal p27 (1:200 dilution, C-19 sc-528, Santa Cruz Biotechnology) Membranes were then incubated with the appropriate secondary antibody for 1 h at room temperature. Immunoreactive proteins were detected using enhanced chemiluminescence (ECL, Santa Cruz Biotechnology).

PowerBlot analysis. For the PowerBlot analysis (high-throughput Western blot screening), A549 cells were treated with ethanol control or resveratrol (25 μmol/L) for 48 h. Following treatment, cells were incubated in lysis buffer [10 mmol/L Tris (pH, 7.4), 1 mmol/L sodium orthovanadate, 1% SDS]. The lysates were passed 10 times through a 25-gauge needle to sheer the cellular DNA. Samples were frozen at −80°C and analyzed by BD Biosciences Transduction Laboratories. The lysates were separated on high-resolution gradient gels and transferred onto nitrocellulose membranes. Each membrane was divided into 40 lanes by applying a chamber-forming grid. To each chamber, a mixture of monoclonal antibodies was added (BD Biosciences Transduction Laboratories). After 1 h of incubation at room temperature, the membranes were rinsed and incubated with secondary antibodies. Resulting images from the Western blot screening were acquired with an IR scanner (Li-Cor), and the molecular mass of each band was assessed using specialized software at BD Biosciences Transduction Laboratories and recognized by an individual antibody in the specific antibody cocktail used. Control and resveratrol samples were run in triplicate. The data received from BD Biosciences Transduction Laboratories was scrutinized in our laboratory and was found to be accurate. Biological processes were analyzed with the PANTHER (Protein Analysis through Evolutionary Relationships) pathway analysis (22). Each protein was categorized and inputted into PANTHER using its associated Locus Link gene identification number. Proteins that met the fold change cutoff of 1.25 and whose associated locus link ID was associated with a biological process with a known GO identification number were considered for analysis by PANTHER.

RNA isolation, microarray analysis, and real-time reverse transcription-PCR. A549 cells were treated with ethanol control or 25 μmol/L resveratrol for 48 h. One replicate of control cells and three replicates of resveratrol-treated cells were analyzed. At the 48-h time point 1 mL TRIzol was added to each culture flask and incubated, and insoluble material was removed by centrifugation at 10,000 rpm for 10 min at 4°C. RNA was isolated and precipitated by mixing with isopropanol (0.8 mL) and centrifuging at 10,000 rpm for 10 min at 4°C. The RNA pellet was washed with 75% ethanol, dried, and dissolved in Rnase-free water. Cleanup of the RNA was done using an RNeasy spin column (Qiagen). The control sample and three treated samples were hybridized to the Human Genome U133 Plus 2.0 arrays (Affymetrix) by the University of Chicago's Functional Genomics Facility. In GeneSpring v7.2 (Agilent Technologies), cell files were preprocessed using the robust multichip average (RMA), genes were normalized to the mean expression of the control sample, and detection cells were used to filter for probe sets present of marginal in one-fourth of the arrays. Fold change values for each experimental sample were exported to Excel for mean and SD calculations. Canonical pathways were analyzed through the use of the software package Ingenuity Pathway Analysis (IPA).[1] Genes from that data set that met the fold change cutoff of 1.2 and were associated with a canonical pathway in the IPA knowledge base were considered for the analysis. Biological processes were analyzed with PANTHER. Genes that met the fold change cutoff of 1.2 and were associated with a biological process with a known GO identification number were considered for analysis.

Total RNA extraction and the RT reaction were done as described previously (24). RNA was further subjected to DNase I (Ambion) digestion and purification using an RNease Mini Kit (Qiagen) before the RT reaction. Real-time PCR was done with 2 μL diluted RT product in a MyiQ Real-time PCR Detection System (Bio-Rad) using iQTM SYBR Green PCR Supermix (Bio-Rad) according to manufacturer's guidelines. The PCR cycling conditions used were (15 s at 95°C, 15 s at 60°C, and 20 s at 72°C) for 40 cycles. Fold inductions were calculated using the formula $2^{-(\Delta\Delta Ct)}$, where $\Delta\Delta Ct$ is $\Delta Ct_{(treatment)} - \Delta Ct_{(control)}$, ΔCt is $Ct_{(target\ gene)} - Ct_{(actin)}$ and Ct is the cycle at which the threshold is crossed. The gene-specific primer pairs (and product size) for the genes analyzed are as follows: Smad2 forward 5′-GGAATTTGCTGCTCTTCTGG-3′ and reverse 5′-TCTGCCTTCGGT-ATTCTGCT-3′(125 bp), Smad3 forward 5′-GGGCTCCCTCATGTCATCTA-3′ and reverse 5′-TTGAAGGCGAACTCACACAG-3′ (98 bp), Smad4 forward 5′-GATACGTGGACCCTTCTGGA-3′ and reverse 5′-ACCTTTGCCTATGTG-CAACC-3′ (104 bp), Smad7 forward 5′-CCAACTGCAGACTGTCCAGA-3′ and reverse 5′-CAGGCTCCAGAAGAAGTTGG-3′ (106 bp), p21 forward

---

5′-GGAAGACCATGTGGACCTGT-3′ and reverse 5′-GGCGTTTGGAGTGG-TAGAAA-3′ (146 bp), p53 forward 5′-AGGCCTTGGAACTCAAGGAT-3′ and reverse 5′-TTATGGCGGGAGGTAGACTG-3′ (106 bp), p27 forward 5′-CCGGCTAACTCTGAGGACAC-3′ and reverse 5′-TTGCAGGTCGCTTCCT-TATT-3′ (106 bp), and β-actin forward 5′-CTCTTCCAGCCTTCCTTCCT-3′ and reverse 5′-AGCACTGTGTTGGCGTACAG-3′ (116 bp). PCR product quality was monitored using post-PCR melt curve analysis.

Results

Resveratrol inhibits growth of A549, NCI H460, and NCI H23 cells in a dose-dependent manner. The effects of various concentrations of resveratrol (1–100 μmol/L) on cell proliferation were examined on A549, NCI H460, and NCI H23 human lung cancer cells. Resveratrol mediated growth inhibition of A549 cells in a dose-dependent manner (Fig. 1*A*), significantly inhibiting growth at 25 μmol/L after a 48-h incubation (IC$_{50}$, 50 μmol/L) as shown by crystal violet assay. A linear growth inhibition was observed up to 100 μmol/L resveratrol, and thereafter, no significant difference in growth inhibition was shown. Additionally, several grapeseed extract–derived compounds (25) did not significantly inhibit cell proliferation (data not shown). Similar effects were also evident in NCI H460 and NCI H23 human lung

cancer cell lines, with resveratrol being the only compound to significantly inhibit cellular growth (Fig. 1*A*).

Effects of resveratrol on the cell cycle progression. To determine the phase of the cell cycle at which resveratrol exerts its growth-inhibitory effect, A549 cells were treated with resveratrol, stained with propidium iodide, and analyzed by flow cytometry. The effect of resveratrol (25 μmol/L for 48 h) on cell cycle progression is shown in Fig. 1*B*. Resveratrol arrested A549 lung cancer cells in the G$_1$ phase of the cell cycle: 70% of A549 cells were found in the G$_1$ phase after 48 h resveratrol treatment in comparison to only 50% of control cells observed to be in G$_1$ after 48 h.

Effects of resveratrol on the induction of apoptosis. Three separate assays were used to investigate the induction of apoptosis in A549 cells by resveratrol (Fig. 1*C*). The cells were treated for 48 h with 25 μmol/L resveratrol and analyzed for apoptosis by the terminal nucleotidyl transferase–mediated nick end labeling (TUNEL), Poly Caspases FLICA, and Mito-PT assays. Resveratrol treatment induced features characteristic of apoptosis as shown by the TUNEL assay [Fig. 1*C(i)* and *(ii)*]. These apoptotic features include brown-stained fragmented nuclei, irregular-shaped cells, and irregular cytoplasmic membranes observed in the
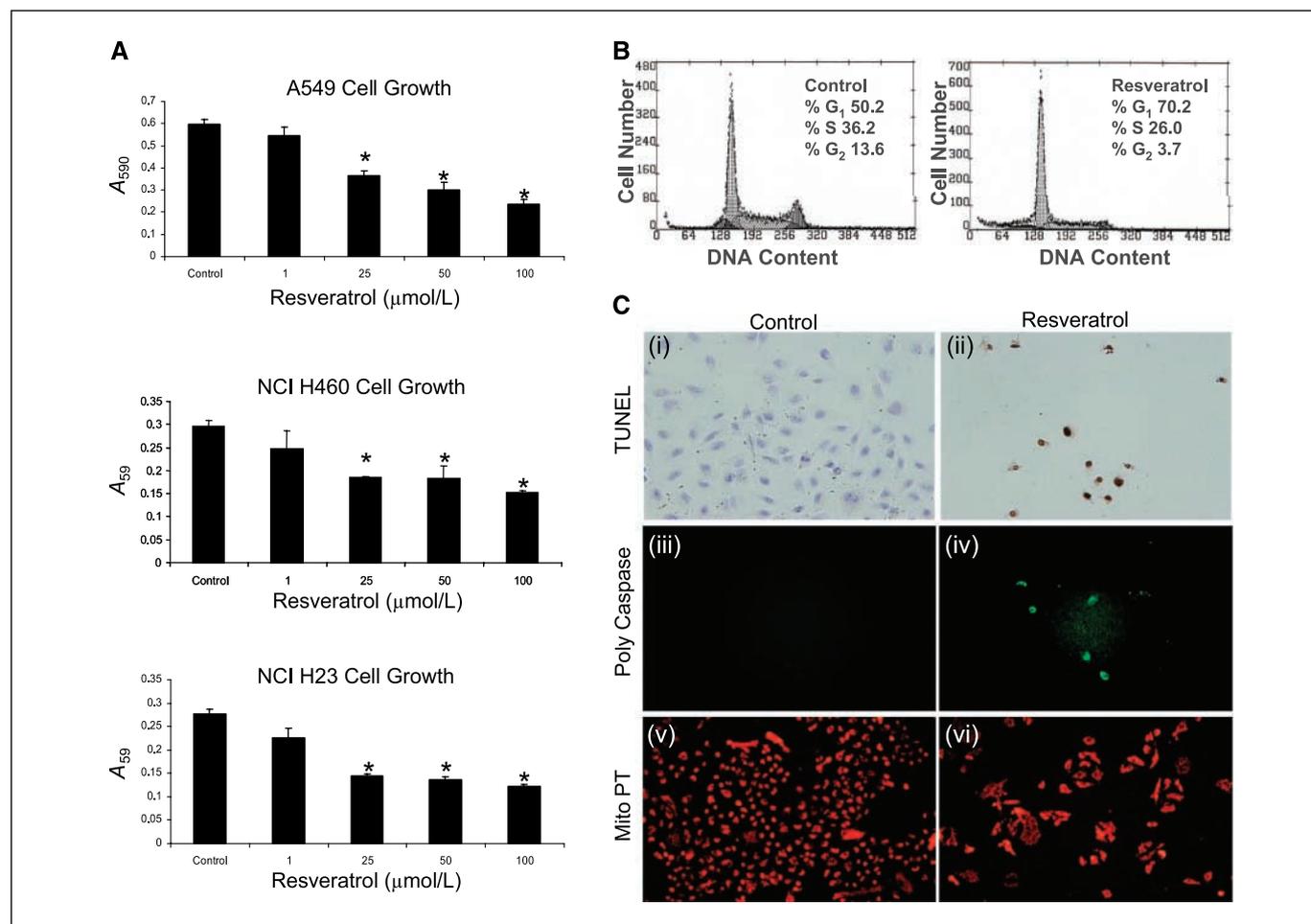

Figure 1. *A,* the dose response of resveratrol (0–100 μmol/L) on A549, NCI H460, and NCI H23 cells after 48 h treatment was determined by crystal violet (*P* < 0.01). *B,* arrest of A549 cells in the G$_1$ phase of the cell cycle after treatment with resveratrol (25 μmol/L) for 48 h as assayed by propidium iodide staining and FACS analysis. *C,* induction of apoptosis by resveratrol (25 μmol/L) in A549 cells after 48 h treatment was determined by the TUNEL Assay (*i* and *ii*), the Poly Caspase FLICA Assay (*iii* and *iv*), and the Mito-PT Assay (*v* and *vi*). Magnification, 20×.

resveratrol-treated cells [Fig. 1C(*ii*)]. The Poly Caspases FLICA assay was used to determine apoptosis via active caspases [Fig. 1C(*iii*) and (*iv*)]. A green fluorescent signal within the cell indicates that an active caspase has formed a covalent bond with the FLICA probe. As can be seen from Fig. 1C(*iv*), A549 cells treated with resveratrol fluoresce green, hence illustrating apoptosis by the activation of the caspase cascade. The Mito-PT assay [Fig. 1C(*v*) and (*vi*)] was used to test for mitochondrial functionality and non–caspase-mediated apoptosis with the Mito-PT reagent. Non-apoptotic healthy control cells [Fig. 1C(*v*)] exhibit red aggregates inside intact mitochondria. Apoptotic resveratrol-treated cells, however, are observed at varying stages of mitochondrial permeability and are identified as the Mito-PT reagent is dispersed throughout the cells [Fig. 1C(*vi*)].

Effects of resveratrol on the expression of *p53, p21,* and *p27* mRNA and protein. We next examined the expression changes of mRNA and proteins that are known to be involved in the inhibition of cell cycle and the induction of apoptosis. Changes in p53, p21, and p27 at both the mRNA and protein levels were studied by real-time reverse transcription-PCR (RT-PCR) and Western blot analysis, respectively. Results showed an accumulation of p53 in resveratrol (25 μmol/L)–treated A549 cells, with a 1.62-fold increase in *p53* mRNA levels over control levels by real-time RT-PCR (Fig. 2*A*). This increase in *p53* mRNA levels was accompanied by an increase in p53 protein levels observed in total cell lysates (Fig. 2*B*). This could be seen as early as 48 h, and the p53 protein level remained elevated to 96 h (Fig. 2*B*). p53 up-regulation within the cell induces p21 expression, which can lead to a p21-mediated inhibition of cyclin D/cyclin-dependent kinase (cdk) and arrest in G$_1$. A *p21* mRNA up-regulation of 6.81-fold over the control mRNA was seen in the resveratrol-treated A549 cells (Fig. 2*C*). p21 protein levels also increased from 24 to 96 h as can be seen in Fig. 2*D*. Although we observed a 1.62-fold up-regulation in *p27* at the mRNA level after resveratrol treatment, this up-regulation was not seen at the protein level (data not shown).

Protein screening by high-throughput Western blot (Power-Blot). A large-scale Western blot–based screening process was employed to identify new targets of resveratrol modification from a group of well-characterized signal transduction proteins. Proteins in the form of total cell lysates were purified from control and resveratrol-treated (25 μmol/L, 48 h) A549 cells and analyzed by PowerBlot analyses. The assay uses 996 individual monoclonal antibodies, of which 841 cross-react with human proteins. Computer-assisted and subsequent manual examination of detected signals revealed 653 protein bands from the PowerBlot screening. When control expression of protein was compared with the protein expression in resveratrol-treated cells, 170 protein bands were identified to be differentially expressed. Based on the confidence with which the identity of the proteins could be deduced, the results were further categorized as follows: Bands that passed a computer-assisted analysis and also passed a manual (visual) positive in all nine of nine comparisons were grouped by specific fold change. One hundred and twenty seven protein bands had a fold change of 1.25 or higher, whereas 89 protein bands had a fold change of 1.5 or higher. These 89 proteins that were altered by resveratrol treatment in A549 cells are listed, along with their specific fold change, respective function, and gene-related locus link identification in Table 1.

Gene expression changes. Using the Affymetrix human genome U133 Plus Array, we screened more than 47,000 transcripts for alterations in A549 mRNA expression after resveratrol treatment (GEO accession number GSE9008). A549 mRNA was harvested after 48 h resveratrol treatment at 25 μmol/L. When compared with the untreated control group, 5,916 genes were found to have altered expression levels of 1.2-fold or more in the resveratrol-treated group. When the fold change cutoff was raised to 1.5-fold, 946 genes were found to have altered expression levels in the resveratrol-treated group. One hundred and fifty-seven genes had fold changes greater than 2-fold.

Using the 1.2-fold change cutoff, the 5,916 genes were imported into Ingenuity Pathway Analysis 4.0. This enabled the identification of biological mechanisms, pathways, and functions most relevant to the genes of interest altered by resveratrol treatment in A549 cells. We identified an array of canonical pathways regulated by

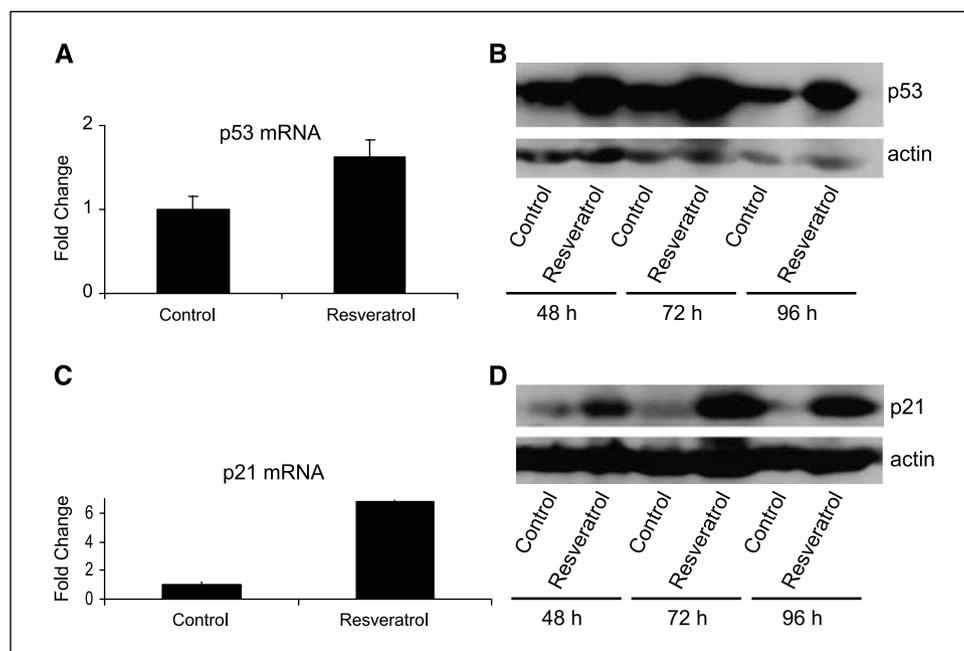**Figure 2.** Regulation of p53 and p21 mRNA and protein levels in A549 human lung cancer cells by resveratrol (25 μmol/L). mRNA levels were analyzed by real-time PCR at 48 h (*A* and *C*). Protein levels were monitored by Western blot analyses over a 96-h time period (*B* and *D*).

Table 1. Alterations in protein expression in A459 cells by resveratrol

Protein ID	Protein function/related information	Locus link ID	Fold change
ADAM9/MDC9	A disintegrin and metalloprotease domain involved in cell-cell and cell-matrix adhesion and possibly the degradation of the extracellular matrix	8754	+2
Annexin II	Substrate for the src oncogene, associated with membrane trafficking	302	+2
A-Raf	Proto-oncogene, serine/threonine-specific protein kinase	64363	+2
ASS	Argininosuccinate synthetase, critical for normal urea cycle function and for basal and inducible NO production	445	+2
Bet1	Golgi integral membrane protein, helps mediate ER to Golgi vesicular transport	29631	+2
BiP/GRP78	Chaperone of the ER lumen, ensures movement of proteins from the ER to the Golgi apparatus	3309	+2
CD38	Cell surface protein, important for lymphocyte migration, and may be involved in the propagation of leukemic cells	952	+2
Doublecortin	Integral component of tyrosine kinase signal transduction pathways that regulate neuronal migration and development of the cerebral cortex	13193	+2
eIF-5a	Eukaryotic initiation factor 5a, role in nuclear transport	1984	+2
Gap1m	GTPase-activating protein 1m, associated with the non-oncogenic form of Ras	25597	+2
Inhibitor 2	A chaperone for protein phosphatase 1, prevents the unregulated dephosphorylation of cellular substrates	5504	+2
Integrin a2/VLA-2a	Role in cellular adhesion, may function in intracellular signal transmission	3673	+2
Phospholipase Cd1	Hydrolyzes inositol phospholipids	5333	+2
PI3K	Phosphorylates the inositol ring of phosphatidylinositol	5295	+2
Rap2	Member of the Ras family of low-molecular-weight GTP/GDP binding proteins	5911	+2
RBP	Retinol-binding protein, transporter of retinol in plasma	5973	+2
Sam68	*Src*-associated in mitosis 68 kDa, functions in mitosis	10657	+2
UbcH7	Ubiquitin-conjugating enzyme H7, involved in the degradation and regulation of proteins in the cell cycle	7332	+2
Ufd2/E4	Ubiquitin-activating enzyme, role in protein degradation	9354	+2
VAP33	May be involved in trafficking of plasma membrane proteins to intracellular sites	9218	+2
Bcl-x	Bcl-2–related protein	598	+1.5
Cathepsin D, 30 kDa	Proteolytic protein, involved in breast cancer pathogenesis, tissue remodeling, tumor invasion	1509	+1.5
CRP1	Cysteine-rich protein 1, regulator of actin cytoskeletal organization	13007	+1.5
Frabin, 115 kDa	Actin cytoskeleton reorganization	246174	+1.5

(*Continued on the following page*)

Table 1. Alterations in protein expression in A459 cells by resveratrol (Cont'd)

Protein ID	Protein function/related information	Locus link ID	Fold change
GCF2	RNA-cytoskeleton interactions, transcriptional repression	8141	+1.5
MCM	Methylmalonyl-CoA mutase, involved in amino acid and fatty acid catabolism	4594	+1.5
mEPHX	Microsomal epoxide hydrolase, involved in epoxide metabolism	2052	+1.5
p116Rip	Thought to participate Rho activation	10928	+1.5
53BP2	p53 binding protein	7159	−1.5
AIB-1	Coactivator of nuclear receptors	8202	−1.5
Caspase-8	Apoptosis-associated protein	841	−1.5
CDC25B	cdc2 tyrosine phosphatase, involved in initiation of apoptosis	994	−1.5
Cyclin A	Mitotic cyclin, activates Cdk2 near the start of S phase, necessary for initiation of DNA replication	890	−1.5
Extracellular signal-regulated kinase (ERK) 2	Serine/threonine kinase, phosphorylates MEK (MAPK/ERK kinase) which, in turn, activates ERK	116590	−1.5
FAK (pY397)	Focal adhesion kinase (FAK), a cytoplasmic tyrosine kinase that colocalizes with integrins in focal adhesions	5747	−1.5
hPrp16	RNA-dependent ATPase, critical for spliceosomal function in the process of pre-mRNA splicing	9785	−1.5
Hsp70	Heat shock/stress-induced gene	3303	−1.5
MSH6/GTBP	DNA mismatch repair involvement	2956	−1.5
p160	Modulates c-Myb–mediated target gene activation	10514	−1.5
p190	Ras-GTPase-activating protein (GAP) associated protein, target of growth factor receptors	394	−1.5
p38 (pT180/pY182)	p38 MAPKs, central kinases in multiple signal transduction pathways	1432	−1.5
pan-JNK/stress-activated protein kinase 1 (SAPK-1)	Phosphorylates multiple transcription factors, induces proinflammatory cytokines	5602	−1.5
PKCi	Member of protein kinase C (PKC) family of homologous serine/threonine protein kinases, involved in cell growth, differentiation, and cytokine secretion	5584	−1.5
Plakophilin 3	Cell adhesion–related protein, involved in desmosomal structure, may have additional nuclear functions	11187	−1.5
ROCK-I/ROKb	Rho-associated serine/threonine kinase, regulation of focal adhesion and stress fiber formation	6093	−1.5
Stat1 (NH$_2$ terminus)	Cytoplasmic signal transducer, activator of transcription	6772	−1.5
Stathmin/metablastin	Regulates microtubule formation during interphase	3925	−1.5
Tim23	Integral membrane component of mitochondrial protein translocation	10431	−1.5
Acetylcholine receptor b	Functions in neurotransmission	24261	−2
Adaptin d	Vesicle transport involvement	8943	−2
Annexin XI	Multiple cytoplasmic and nuclear functions	11744	−2
B2 bradykinin receptor	Neurobiological receptor	624	−2
β-Dystroglycan	Neuromuscular junction associated protein	1605	−2
B56a	Reversible phosphorylation phosphatase	5525	−2
BUBR1	Mitotic spindle checkpoint activation	701	−2
Caspase-2/ICH-1L	Apoptosis	835	−2
CDC27	G$_2$-M cell cycle transition	996	−2
Cdk1/Cdc2	M-phase cell cycle transition	983	−2
C-Raf	Ser/Thr kinase growth factor response	7187	−2
CRIK	Citron Rho-interacting kinase	11113	−2
Cyclin B	Mitotic protein kinase, subunit for cdk1/cdc2	891	−2
Cyclin D3	G$_1$ cell cycle transition	896	−2
Desmoglein	Transmembrane glycoprotein found in desmosome junctions	1828	−2
E-Cadherin	Epithelial cell junction/adhesion function	999	−2

Table 1. Alterations in protein expression in A459 cells by resveratrol (Cont'd)

Protein ID	Protein function/related information	Locus link ID	Fold change
Eg5	Mitotic spindle motor protein	3832	−2
GIT2-short	GTPase activation of ADP ribosylation factor (ARF)	9815	−2
Glucocorticoid receptor	Steroid hormone receptor	2908	−2
Heme oxygenase 1	Function in heat/oxidative/endotoxic cell stress	3162	−2
ICBP90	DNA topoisomerase–related protein	29128	−2
Integrin a5	Cell-cell/cell matrix adhesion	3678	−2
IRS-1	Insulin receptor substrate (insulin-induced signal transduction)	25467	−2
Karyopherin a/Rch-1	Nuclear localization of cytosolic proteins	3838	−2
MAP4	Microtubule-associated protein/assists in microtubule stabilization	4134	−2
NAT1	Protein translation	1982	−2
Nestin	Intermediate filament protein	10763	−2
OPA1	Putative role in mitochondrial biogenesis	4976	−2
PBK	MAP kinase signal transduction	55872	−2
RanBP3, 80 kDa	GTPase mitosis, nuclear transport, DNA replication	8498	−2
RECK	Reversion-inducing cysteine-rich protein with Kazal motifs	8434	−2
Reps1	Function in epidermal growth factor (EGF) receptor tyrosine kinase complexes	85021	−2
s3A	Involved in trans Golgi protein trafficking	6189	−2
Smad2/3, 55 kDa	TGF-β signaling response	4088	−2
Smad2/3, 61 kDa	TGF-β signaling response	4087	−2
SRPK1	Pre-mRNA splicing	6732	−2
TIEG2	Sp1-like transcription factor family member (repression of gene transcription/inhibition of cell growth)	8462	−2
V-1/myotrophin	Granule cell differentiation	136319	−2
VASP	Substrate for cyclic AMP-/cyclic guanosine 3′,5′-monophosphate-dependent kinases, associated with actin filaments, focal adhesions, and dynamic membrane regions	7408	−2
VHR	Phosphatase regulation of cyclin-dependent kinases during the cell cycle	1845	−2

NOTE: Proteins with a change in expression greater than 1.5-fold as determined by PowerBlot analysis are represented. Each protein passed a computer-assisted analysis and also passed a manual positive fold change check in all nine out of nine comparisons. Locus link gene identifications assigned to each PowerBlot protein and an associated protein function column are also shown.

resveratrol in human lung cancer cells. The G$_1$-S cell cycle checkpoint pathway was a canonical pathway identified by Ingenuity to be altered by resveratrol action. This correlated with our previous findings above. In addition, the G$_2$-M cell cycle checkpoint pathway, as well as the apoptosis cell death cascade pathway, was identified to be altered by resveratrol treatment in A549 cells. The identification of gene alterations in the transforming growth factor-β (TGF-β) pathway was identified by the microarray screen and highlighted by Ingenuity as shown in Fig. 3. The TGF-β pathway activators, *Smad2*, *Smad3*, and *Smad4* were found to be down-regulated by resveratrol, whereas the TGF-β pathway repressor *Smad7* was found up-regulated at the mRNA level. Down-regulation of mRNAs for *Smad2* and *Smad4* and the up-regulation of mRNA for *Smad7* were further ascertained by real-time PCR (Fig. 3*B*). Immunofluorescence results using antibodies against each of the Smad proteins suggest the up-regulation of Smad7 protein expression and the down-regulation of nuclear Smad2 and Smad4 in A549 cells after resveratrol treatment, which is in accordance with the microarray and RT-PCR results (data not shown). In addition, canonical pathways of the NF-κB pathway and

the p38 mitogen-activated protein kinase/c-jun-NH$_2$-kinase (MAPK/JNK) signaling pathway were also altered by resveratrol.

Combined analysis of PowerBlot and Microarray results. The PANTHER classification system is a large database of protein families that have been subdivided into functionally related subfamilies. Proteins are classified into families of shared function, which are then categorized by molecular function and biological process ontology terms (26).

We analyzed the microarray results with PANTHER using a 1.2-fold change cutoff and categorized the mRNA changes into biological processes. Similarly, substituting the Locus Link gene ID for each of the PowerBlot proteins, we introduced the results of the PowerBlot using the 1.25-fold change cutoff (127 proteins) and categorized these changes into biological processes. Each biological process has been determined by PANTHER from ontologies similar to "GO Gene Ontologies"; however, the PANTHER biological processes are simplified to allow for high-throughput analyses. Our results show that the top biological processes found in the gene array complemented those found in the PowerBlot analysis (Table 2). When considering both microarray and PowerBlot
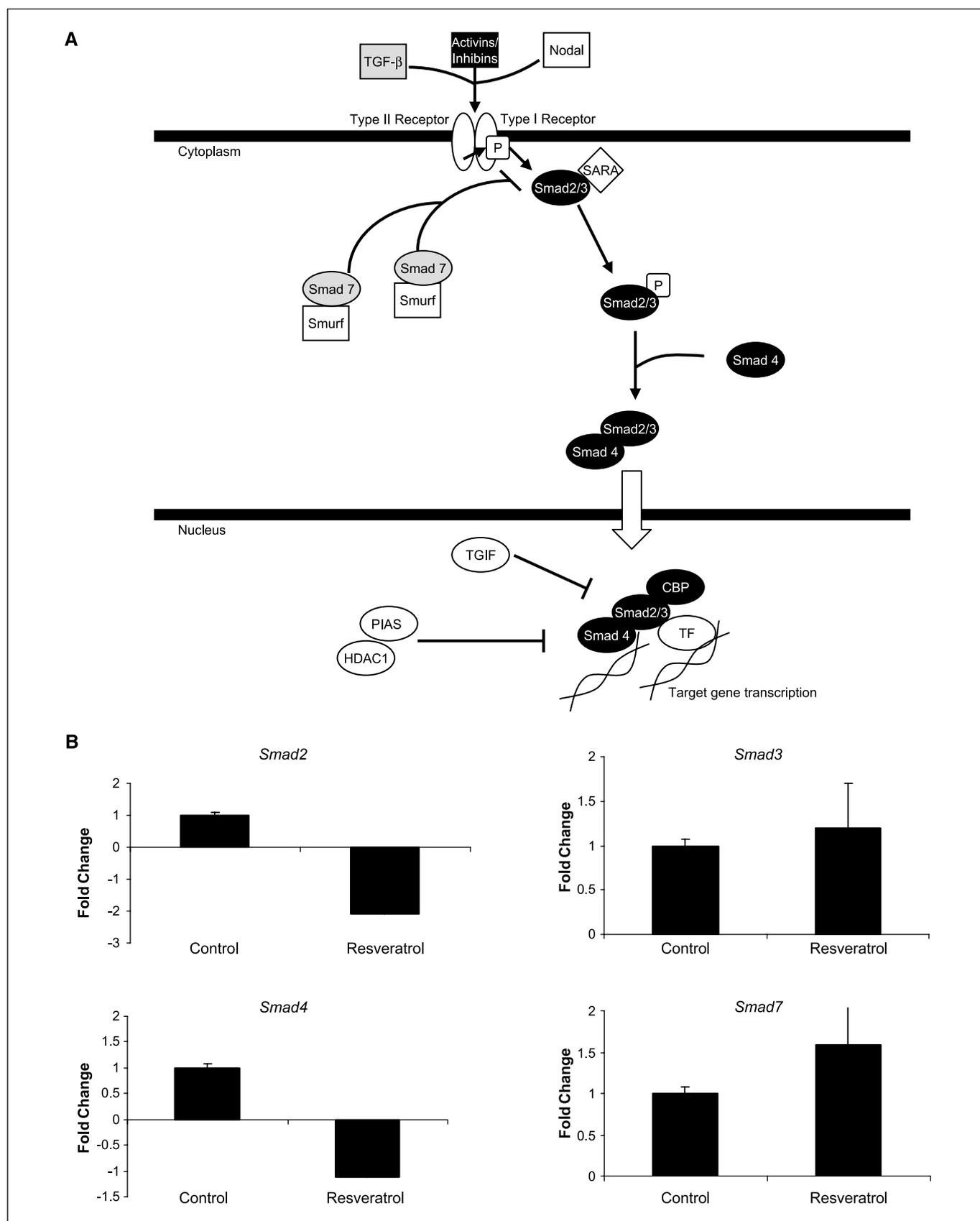
Figure 3. *A,* microarray data illustrating gene alterations (>1.2-fold) in the TGF-β pathway by resveratrol (25 μmol/L for 48 h) in A549 cells as analyzed by Ingenuity pathway analysis. *Black,* up-regulation. *Gray,* down-regulation. *B,* mRNA levels of *Smad2, Smad3, Smad4,* and *Smad7* as analyzed by real-time PCR in resveratrol-treated (25 μmol/L for 48 h) A549 cells.

Table 2. Biological processes altered by resveratrol in A549 cells

Biological process	Microarray genes	PowerBlot proteins	GO ID	Panther ID
Nucleoside, nucleotide, and nucleic acid metabolism	615	17	0006139	BP00031
Protein metabolism and modification	522	31	0019538	BP00060
Signal transduction	510	31	0007165	BP00102
Developmental processes	342	15	0007275	BP00193
Immunity and defense	213	10	0006952	BP00148
Intracellular protein traffic	210	9	0006886	BP00125
Cell structure and motility	198	9	0007010	BP00285
Transport	193	7	0006810	BP00141
Cell cycle	187	19	0006810	BP00203
Cell proliferation and differentiation	186	13	0008283	BP00224
Lipid, fatty acid, and steroid metabolism	138	2	0006629	BP00019
Carbohydrate metabolism	115	3	0005975	BP00001
Apoptosis	112	11	0006915	BP00179
Other metabolism	109	4	0008152	BP00289
Oncogenesis	92	8	NA	BP00281
Cell adhesion	92	8	0007155	BP00124
Neuronal activities	72	2	0019226	BP00166
Amino acid metabolism	59	1	0006520	BP00013
Protein targeting and localization	47	4	0006615	BP00137
Homeostasis	42	0	0019725	BP00267
Sensory perception	33	1	0007600	BP00182
Electron transport	31	0	0006118	BP00076
Coenzyme and prosthetic group metabolism	28	1	0051186	BP00081
Muscle contraction	28	1	0006936	BP00173
Sulfur metabolism	23	0	0006790	BP00101
Phosphate metabolism	20	3	0006796	BP00095
Blood circulation and gas exchange	9	1	0008015	BP00209
Nitrogen metabolism	8	2	0006807	BP00090
Non-vertebrate process	3	0	NA	BP00301

NOTE: Gene and protein changes were inputted into PANTHER using locus link identifications, and top biological processes were compared. Biological processes are identified by known GO and PANTHER identification numbers.

results, the top biological processes altered by resveratrol in A549 cells were those of nucleic acid metabolism, protein metabolism, cell cycle, and cell proliferation/differentiation signaling pathways. The proteins/genes that belong to these PANTHER categorized biological processes include a long list of macromolecules (data not shown).

Due to the fact that the top biological processes altered by resveratrol in A549 cells were similar at both the mRNA and protein levels, we focused on the specific genes/proteins regulated in these processes. Specifically, for each individual PowerBlot protein that was identified to be altered by resveratrol, we determined whether its corresponding mRNA was also affected in the same manner as assayed by the microarray. Comparing the microarray and PowerBlot results using a fold change cutoff of 1.2-fold for both the microarray and PowerBlot, we identified 23 genes/proteins that were regulated in a similar manner (Table 3). These analyses revealed genes/proteins, including cyclins, phosphoinositide-3 kinase (PI3K), Eg5, ASS, Chk1, integrins, FAK, and others that were modulated by resveratrol. Thus, the approach of combining genes/protein expressions provides a selective and highly informative list to identify signaling pathways for mechanism(s) of chemopreventive and/or chemotherapeutic agents such as resveratrol.

Discussion

The functional activities of a protein, such as substrate phosphorylation and levels of activated protein, are arguably the best estimate of biological activity in a given cellular system (27, 28). Besides these, a highly valued and accepted form of analysis of biological activity is an estimate of the actual levels of mRNA or protein within a cell. In this study, we have undertaken a combined experimental approach to understand the biological activity and molecular mechanisms of resveratrol in A549 lung cancer cells. Using the high-throughput techniques of both microarray and PowerBlot, we measured mRNA and protein expression, respectively. These techniques, when combined, generated a large body of biological data, which, when evaluated, provided new insights into the molecular mechanisms of resveratrol action in human lung cancer.

In this report, we observed that resveratrol induces gene and protein expression involved in multiple biological processes in A549 lung cancer cells (Table 2). Many of the gene/protein expression changes such as the up-regulation of p53 and p21 and the activation of the caspases identified in the present report have been reported previously. In addition, we also report new signaling pathways as identified from the gene array and PowerBlot analyses in A549 cells.

The roles of resveratrol both as a chemopreventive as well as a chemotherapeutic agent have previously been reported (29). These growth-suppressing properties are confirmed for A549 cells in this report. The flow cytometry analyses suggested that resveratrol arrested cells in the G_1 phase. Previous studies, on the other hand, have reported that resveratrol or its related stilbenoids arrested cells in the S or G_2-M phases of the cell cycle (21). The changes in both gene and protein expression, such as the up-regulation of p53 and p21 and the down-regulation of cyclin A, chk1, CDC27, and Eg5 (a mitotic motor protein; see Tables 1 and 3) indicate that resveratrol may have a regulatory role both in G_1 as well as in the S and G_2-M phases of the cell cycle. Furthermore, the microarray results, when analyzed by Ingenuity Pathway Analysis, also indicated that resveratrol mediated alterations in both the G_1 and the G_2-M cell cycle canonical pathways. In the literature, reports indicate that resveratrol affects different stages of the cell cycle depending on the cancer cell type. The significance of differential regulation by resveratrol in different tissue types is not clear (1). However, chemopreventive agents have been known to show target organ specificity and different modes of action.

We have used two novel assays to determine the route of apoptosis in A549 cells by resveratrol. The poly caspase FLICA and the Mito-PT assays verify the activation of the caspase and the loss of the mitochondrial permeability transition, respectively. These results are consistent with previously reported results in A549 cells (20, 25) and in cancer cells of other organs such as breast, colon, and leukemia (1).

The present study highlights the findings of resveratrol action on the TGF-β pathway, particularly the Smad proteins (Fig. 3). TGF-β binds to both types I and II receptors (TGF-β-RI and TGF-β-RII),

respectively. TGF-β-RII is constitutively active and phosphorylates TGF-β-RI. TGF-β-RI, in turn, activates the receptor-regulated Smad proteins, Smad2 and Smad3, whereas Smad5 and Smad8 are regulated by bone morphogenetic proteins. There are a number of mutations identified in human tumors, many of which result in the loss of selective Smad proteins. This ultimately alters TGF-β signaling. TGF-β plays a crucial role in tissue homeostasis through the activation of the intracellular Smad proteins (30). The Smad transcription factors and Smad-ubiquitin regulatory factor (Smurf1) are involved in early embryonic morphogenesis of lungs (31). However, the role of Smads and TGF-β signaling pathways has not been reported in lung carcinogenesis or its prevention or treatment (32, 33). Furthermore, alterations in the TGF-β pathway affecting Smad proteins by resveratrol have not been investigated. We illustrate that at the mRNA level, the Smad activators, *Smad2* and Smad4 are down-regulated, and that the repressor *Smad7* is up-regulated following resveratrol treatment. Consistently, the PowerBlot results showed the down-regulation of *Smad2/3* at the protein level. We hypothesize that this altered regulation of the Smads leads to a block in the nuclear signaling of the TGF-β pathway, which, in turn, results in the inhibition of A549 cell proliferation.

Using this dual microarray-PowerBlot approach, we examined the pathways of resveratrol-induced gene and protein expression with two software packages, Ingenuity Pathway Analysis and PANTHER. The pathway results of the microarray complimented those of the PowerBlot and vice versa (Table 2). Results showed that altered expression changes matched between the microarray and PowerBlot in a total of 23 genes/proteins that were on both templates (Table 3). The discrepancies between the microarray

Table 3. Gene and protein changes with equivalent fold change directions after resveratrol treatment in A549 cells as assayed by microarray and PowerBlot analysis

Protein name	Gene ID	Microarray fold change	PowerBlot (control, treated)
Glucocorticoid receptor	2908	−1.71	
FAK (pY397), phospho-specific	5747	−1.58	
Hsp70	3303	−1.45	
LITAF	9516	−1.44	
AIB-1	8202	−1.41	
p190	394	−1.35	
Stat1	6772	−1.32	
Smad2/3, 55 kDa	4087	−1.31	
PRK2	5586	−1.29	
Chk1	1111	−1.26	
ROCK-I/ROKb	6093	−1.25	
Eg5	3832	−1.23	
MSH6/GTBP	2956	−1.23	
CDC27	996	−1.22	
B2 bradykinin receptor, 42 kDa	624	−1.21	
Cyclin A	890	−1.21	
Inhibitor 2	5504	1.21	
CD38	952	1.22	
Integrin a2/VLA-2a	3673	1.23	
mEPHX	2052	1.34	
PI3K	5295	1.46	
Bcl-x	598	1.46	
ASS	445	2.41	

NOTE: Actual raw images from the PowerBlot of control and treated groups are displayed.

(mRNA expression) and PowerBlot (protein expression) techniques could represent altered posttranslational regulation or inherent inaccuracies of these high-throughput techniques.

This *in vitro* study suggests that resveratrol is a potent inhibitor of A549 lung cancer cell growth. A recent *in vivo* study by Berge et al. (34) reported that resveratrol has no preventive effect on benzo(*a*)pyrene-induced lung tumorigenesis in mice. The bioavailability of resveratrol to the lungs after being administered in the diet in this study is probably the factor responsible for this discrepancy. Resveratrol is known to be cleared from tissues rapidly after p.o. administration in mice (35), and it is possible the route/mode of administration needs to be altered for efficacy. Moreover, benzo(*a*)pyrene induces lung adenoma in mice. It is possible that resveratrol may not be efficacious against benign adenoma induction in the lungs in this model. In addition, Berge et al. in this study found no resveratrol or resveratrol conjugates in the lung tissue of the mice following resveratrol treatment.

In conclusion, we have shown that resveratrol alters a large number of genes and proteins and inhibits A549 cell proliferation by inducing cell cycle arrest, inducing apoptosis, and by altering the intracellular Smad signaling of the TGF-β pathway. Although there are additional pathways identified by this combined approach, their description is beyond the scope of this article. Nevertheless, the benefits of using dual high-throughput techniques to unravel the molecular mechanisms of resveratrol is emphasized in this report.

References

1. Aggarwal BB, Bhardwaj A, Aggarwal RS, Seeram NP, Shishodia S, Takada Y. Role of resveratrol in prevention and therapy of cancer: preclinical and clinical studies. Anticancer Res 2004;24:2783–840.
2. Soleas GJ, Diamandis EP, Goldberg DM. Resveratrol: a molecule whose time has come? And gone? Clin Biochem 1997;30:91–113.
3. Terla B, Waterhouse A. Resveratrol: isomeric molar absorptivities and stability. J Agric Food Chem 1996;44: 1253–7.
4. Lopez R, Dugo P, Mondello L. Determination of *trans*-resveratrol in wine by micro-HPLC with fluorescence detection. J Sep Sci 2007;30:669–72.
5. Shimuzu M, Weinstein IB. Modulation of signal transduction by tea catechins and related phytochemicals. Mutat Res 2005;59:147–9.
6. Delmas D, Jannin B, Latruffe N. Resveratrol preventing properties against vascular alterations and aging. Mol Nutr Food Res 2005;49:377–95.
7. Kasdallah-Grissa A, Mornagui B, Aouani E, et al. Resveratrol a red wine polyphenol attenuates ethanol-induced oxidative stress in liver. Life Sci 2007;80:1033–9.
8. Stef G, Csiszar A, Lerea K, Ungarvari Z, Veress G. Resveratrol inhibits aggregation of platelets from high risk cardiac patients with aspirin resistance. Cardiovesc Pharmacol 2006;48:1–5.
9. Bhat KPL, Kosmeder JW II, Pezzuto JM. Biological effects of resveratrol. Antioxid Redox Signal 2001;3: 1041–64.
10. Mehta RG, Pezzuto JM. Phytochemicals as potential cancer chemopreventive agents. In: Bagchi D, Preus HG, editors. Phytopharamceuticals in cancer chemoprevention. CRC Press; 2004. p. 237–46.
11. Jang M, Cai L, Udeani GO, et al. Cancer chemopreventive activity of resveratrol, a natural product derived from grapes. Science 1997;275:218–20.
12. Bhat KP, Pezzuto JM. Cancer chemopreventive activity of resveratrol. Ann N Y Acad Sci 2002;957:210–29.
13. Schneider Y, Vincent F, Duranton B, et al. Antiproliferative effect of resveratrol, a natural component of grapes and wine, on human colonic cancer cells. Cancer Lett 2000;158:85–91.
14. Stewart JR, Artime MC, O'Brian CA. Resveratrol: a candidate nutritional substance for prostate cancer prevention. J Nutr 2003;133:2440–3S.
15. Revel A, Raanani H, Younglai E, et al. Resveratrol, a natural aryl hydrocarbon receptor antagonist, protects lung from DNA damage and apoptosis caused by benzo(*a*)pyrene. J Appl Toxicol 2003;23: 255–61.
16. Signorelli P, Ghidoni R. Resveratrol as an anticancer nutrient: molecular basis, open questions and promises. J Nutr Biochem 2005;16:449–66.
17. Fulda S, Debatin KM. Resveratrol modulation of signal transduction in apoptosis and cell survival: a mini-review. Cancer Detect Prev 2006;30:217–23.
18. Delmas D, Lancon A, Colin D, Jannin B, Latruffe N. Resveratrol as a chemopreventive agent: a promising molecule for fighting cancer. Curr Drug Targets 2006;7: 423–42.
19. Aziz MH, Kumar R, Ahmad N. Cancer chemoprevention by resveratrol: *in vitro* and *in vivo* studies and the underlying mechanisms (review). Int J Oncol 2003;23:17–28.
20. Benedetti A, Parent ME, Siemiatycki J. Consumption of alcoholic beverages and risk of lung cancer: results from two case control studies in Montreal, Canada. Cancer causes Control 2006;17:469–80.
21. Kim YA, Lee WH, Choi TH, Rhee SH, Park KY, Choi YH. Involvement of p21WAF1/CIP1, pRB, Bax and NF-κB in induction of growth arrest and apoptosis by resveratrol in human lung carcinoma A549 cells. Int J Oncol 2003;23:1143–9.
22. Ahmad N, Adhami VM, Afaq F, Feyes DK, Mukhtar H. Resveratrol causes WAF-1/p21–mediated G(1)-phase arrest of cell cycle and induction of apoptosis in human epidermoid carcinoma A431 cells. Clin Cancer Res 2001; 7:1466–73.
23. Vindeløv LL, Christensen IJ, Nissen NI. A detergent-trypsin method for the preparation of nuclei for flow cytometric DNA analysis. Cytometry 1983;3:323–7.
24. Peng X, Maruo T, Cao Y, et al. A novel RARß isoform directed by a distinct promoter P3 and mediated by retinoic acid in breast cancer cells. Cancer Res 2004;64: 8911–8.
25. Waffo-Teguo P, Hawthorne ME, Cuender M, et al. Potential cancer chemopreventive activities of wine stilbenoids and flavans extracted from grape (*Vitis vinifera*) cell cultures. Nutr Cancer 2002;40:173–9.
26. Thomas PD, Campbell MC, Kejariwal A, et al. PANTHER: a library of protein families and subfamilies indexed by function. Genome Res 2003;13:2129–41.
27. Yoo GH, Piechocki MP, Ensley JF, et al. Docetaxel induced gene expression patterns in head and neck squamous cell carcinoma using cDNA microarray and PowerBlot. Clin Cancer Res 2002;8:3910–21.
28. Narayanan BA Chemopreventive agents alter global gene expression pattern: predicting their mode of action and targets. Curr Cancer Drug Targets 2006;6:711–27.
29. Lee EJ, Min HY, Joo Park H, et al. G$_2$/M cell cycle arrest and induction of apoptosis by a stilbenoid, 3,4,5-trimethoxy-4'-bromo-*cis*-stilbene, in human lung cancer cells. Life Sci 2004;75:2829–39.
30. Bornstein S, Hoot K, Han GW, Lu SL, Wang XJ. Distinct roles of individual Smads in skin carcinogenesis. Mol Carcinog. Epub ahead of print 2007.
31. Shi W, Chen H, Sun J, et al. Overexpression of Smurf1 negatively regulates mouse embryonic lung branching morphogenesis by specifically reducing Smad1 and Smad 5 proteins. Am J Physiol Lung Cell Mol Physiol 2004;286:L293–300.
32. Derync R, Akhurst RJ, Balmin A. TGF β signaling in tumor suppression and cancer progression. Nat Gent 2001;29:117–29.
33. Liu F, Pouponnot C, Massague J. Dual role of Smad 4/DPC4 tumor suppressor in TGFβ inducible transcriptional complexes. Genes Dev 1997;11:3157–67.
34. Berge G, Øvrebø S, Eilertsen E, Haugen A, Mollerup S. Analysis of resveratrol as a lung cancer chemopreventive agent in A/J mice exposed to benzo(*a*)pyrene. Br J Cancer 2004;91:1380–3.
35. Asensi M, Medina I, Ortega A, et al. Inhibition of cancer growth by resveratrol is related to its low bioavailability. Free Radic Biol Med 2002;33:387–98.

Molecular Mechanisms of Resveratrol Action in Lung Cancer Cells Using Dual Protein and Microarray Analyses

Lorna Whyte, Yuan-Yen Huang, Karen Torres, et al.

Updated version	Access the most recent version of this article at: http://cancerres.aacrjournals.org/content/67/24/12007

Cited articles	This article cites 32 articles, 7 of which you can access for free at: http://cancerres.aacrjournals.org/content/67/24/12007.full#ref-list-1
Citing articles	This article has been cited by 3 HighWire-hosted articles. Access the articles at: http://cancerres.aacrjournals.org/content/67/24/12007.full#related-urls

E-mail alerts	Sign up to receive free email-alerts related to this article or journal.
Reprints and Subscriptions	To order reprints of this article or to subscribe to the journal, contact the AACR Publications Department at pubs@aacr.org.
Permissions	To request permission to re-use all or part of this article, use this link http://cancerres.aacrjournals.org/content/67/24/12007. Click on "Request Permissions" which will take you to the Copyright Clearance Center's (CCC) Rightslink site.